

Supporting Information

for

Identification of molecular recognition of Langmuir-Blodgett monolayers using surface-enhanced Raman scattering spectroscopy

Xianming Kong,^{a,b} Qian Yu,^a Zhongpeng Lv,^a Xuezhong Du^{*a} and Tapani Vuorinen^b

^a Key Laboratory of Mesoscopic Chemistry (Ministry of Education), State Key Laboratory of Coordination Chemistry, and School of Chemistry and Chemical Engineering, Nanjing University, Nanjing 210093, People's Republic of China

^b Department of Forest Products Technology, School of Chemical Technology, Aalto University, P.O. Box 16300, FI-00076 Aalto, Finland

E-mail: xzdu@nju.edu.cn

Experimental Section

Chemicals and reagents

Silver nitrate (AgNO_3), sodium citrate ($\text{Na}_3\text{C}_6\text{H}_5\text{O}_7$), melamine (99%), and ethanol were purchased from Sinopharm Chemical Reagent Co., Ltd. (analytical grade), and concentrated hydrochloric acid (HCl) and concentrated nitric acid (HNO_3) from Nanjing Chemical Reagent Co., Ltd. (analytical grade). 3-Aminopropyltrimethoxysilane (APTMS) and *p*-aminothiophenol (PATP, 97%) were obtained from Sigma-Aldrich, and adenosine (97%), thymidine (99%), cytidine (99%), and stearic acid (90–95%) from Fluka. Stearic acid was recrystallized from ethanol twice prior to use. 5-Octadecylbarbituric acid (C_{18}BA) was synthesized according to the method reported previously with a small modification in amount of reactants and volume of solvents.^{S1} The water used was double-distilled (pH 5.6, resistivity of 18.2 M Ω cm, surface tension of 73.06 mN/m at 22 °C) after a deionized exchange.

Synthesis of AgNPs

All glassware used in the following procedures were washed with freshly prepared *aqua regia* (HNO_3/HCl , 1:3, v/v) followed by washing thoroughly with double-distilled water. AgNPs were synthesized according to the Lee and Meisel's method.^{S2} A total of 200 mL of aqueous AgNO_3 solution (1 mM) was heated to boil under vigorous stirring, and then 4 mL of 1% trisodium citrate was rapidly added. The solution quickly turned yellow-green, and continuous stirring proceeded for 1 h. After gradually turning gray-green, the solution was cooled to room temperature under stirring to obtain Ag colloids.

Preparation of AgNP-assembled substrates

The glass slides with the size of 1 cm \times 2 cm were first treated in *piranha* (98% $\text{H}_2\text{SO}_4/30\%$ H_2O_2 , 3:1, v/v) for 30 min to remove organic pollutants followed by washing repeatedly with double-distilled water and ethanol, then were placed in oven to activate at 80 °C for 12 h followed by cooling to room temperature. The glass slides were placed in a beaker (250 mL), and then 80 mL of anhydrous ethanol and 50 μL of APTMS were added for surface functionalization. After 10 h, the amino-functionalized glass slides were taken out followed by

washing with ethanol and double-distilled water, and then were immersed in Ag colloids for assemblies of nanoparticles on the surfaces. After 6 h, the AgNP-assembled glass slides were taken out and then washed with double-distilled water, and finally immersed in double-distilled water prior to use.

Fabrication of LB films

CaF₂, quartz, and glass slides as well as the AgNP-assembled substrates were used for deposition of LB films, respectively. The spreading and transfer of the monolayers were performed on a Nima 611 Langmuir trough with two moving barriers. A Wilhelmy plate (a piece of filter paper) was situated in the middle of the trough and used as the surface pressure sensor. Monolayers were obtained by spreading the chloroform solution of C₁₈BA (1 mM) on aqueous subphases. The subphase temperature was kept at 22 °C. For the deposition of LB films, the monolayers were first compressed to a desired surface pressure of 20 mN/m, and then 30 min was allowed for the monolayers to reach equilibrium. LB monolayer films were transferred onto various substrates by the vertical method at a pulling rate of 2.0 mm/min.

The spreading and transfer of the stearic acid monolayers were carried out on a KSV Langmuir minitrough 2 with two barriers. A Wilhelmy plate of platinum was used as the surface pressure sensor and situated in the middle of the trough. Monolayers were obtained by spreading the chloroform solution of stearic acid (1 mg/mL) on pure water and aqueous PATP subphases (0.5 mM). The other experimental conditions and procedures were the same as those in the case of C₁₈BA.

Instruments and measurements

Raman spectra for the molecular recognition of C₁₈BA and melamine were obtained using a Renishaw InVia Raman spectrometer equipped with a CCD detector, and 50-objective was used for spectral measurements. The excitation wavelength was 514.5 nm from an air-cooled argon ion laser, and the diameters of the lasers were in the range of 1–2 μm. Raman spectrometer was calibrated by a silicon wafer at 520 cm⁻¹ Raman shift before SERS measurement. The exposure times for Raman measurements were 10 s, and SERS spectra were collected by coaddition of 2 scans. Raman spectra for the molecular recognition of

stearic acid and PATP were acquired on an alpha 300RA Combined Confocal Raman and AFM microscope system (WITec, Inc., Ulm, Germany), with the excitation line of 532 nm from a neodymium doped yttrium aluminum garnet (Nd:YAG) laser and 20-objective lens. For the SERS measurements using the ALINERS approach, 3 μL of silver colloids was dripped onto the surface of LB monolayers with a pipette followed by drying in ambient environments. FTIR transmission spectra of the LB films on CaF_2 substrates were recorded on a VERTEX 70V spectrometer (Bruker) with a DTGS detector. Typically 1024 scans were collected to obtain a satisfactory signal-to-noise ratio with the resolution 4 cm^{-1} . The film spectra were obtained by subtracting the spectra of blank CaF_2 substrates from the corresponding sample spectra. UV-vis spectra of LB films on quartz substrates were recorded on a UV-3600 spectrophotometer (Shimadzu), and UV-vis spectra of aqueous solutions were measured on the same spectrophotometer in quartz cells of 1 cm optical path. The transmission electron microscopy (TEM) image of AgNPs was recorded on a JEM-2100 microscope operated at 200 KV, and the atomic force microscopy (AFM) image of the AgNP-assembled silicon wafer pre-immobilized with APTMS was acquired on a Nanoscope IIIa Multimode scanning probe microscopy (Digital Instruments Inc.) with the tapping mode in air. No image processing was performed except flattening.

Density functional theory (DFT) calculations

DFT calculations were performed with M062X,^{S3} CAM-B3LYP,^{S4} B3LYP,^{S5,S6} and PW91PW91^{S7} for finding stable optimization geometries and calculating vibrational Raman spectra. The basis sets for C, N, S, and H were 6-311+G** with polarization functions for C, N, S, and H, and with diffuse function only for C, N, and S atoms. All the calculations concerning the geometry optimization and the Raman spectra were performed by using Gaussian 09 software package.^{S8}

The differential Raman scattering cross-sections, which are proportional to vibrational Raman intensity, can be calculated from the scattering activities and the predicted wavenumbers for each normal mode using the relationship,^{S9}

$$\left(\frac{d\sigma}{d\Omega}\right)_k = \frac{h}{8\pi^2 c \omega_k} \frac{2\pi^4 (\omega_i - \omega_k)^4}{45} S_k \left[1 - \exp\left(-\frac{hc\omega_k}{kT}\right)\right]^{-1}$$

where h , c , and k are universal constants, ω_i is the exciting wavenumber, and ω_k is the vibrational wavenumber of the k_{th} normal mode (both in cm^{-1}), and S_k is the corresponding Raman scattering factor (unit in $\text{\AA}^4/\text{amu}$) that can be directly calculated using Gaussian 09. This formula assumes a particular experimental condition, observation perpendicular to a linearly polarized incoming laser beam. The differential Raman scattering cross-sections and calculated scaled wavenumbers are used together with a Lorentzian line shape function with FWHM of 10 cm^{-1} to obtain the calculated spectrum.

References

- S1 M. Weck, R. Fink and H. Ringsdorf, *Langmuir*, 1997, **13**, 3515–3522.
- S2 P. C. Lee and D. Meisel, *J. Phys. Chem.*, 1982, **86**, 3391–3395.
- S3 Y. Zhao and D. G. Truhlar, *Theor. Chem. Acc.*, 2008, **120**, 215-241.
- S4 T. Yanai, D. P. Tew and N. C. Handy, *Chem. Phys. Lett.*, 2004, **393**, 51-57.
- S5 C. T. Lee, W. T. Yang and R. G. Parr, *Phys. Rev. B*, 1988, **37**, 785-789.
- S6 P. J. Hay and W. R. Wadt, *J. Chem. Phys.*, 1985, **82**, 299-310.
- S7 J. P. Perdew, J. A. Chevary, S. H. Vosko, K. A. Jackson, M. R. Pederson, D. J. Singh and C. Fiolhais, *Phys. Rev. B*, 1992, **46**, 6671-6687.
- S8 M. J. Frisch, G. W. Trucks, H. B. Schlegel, G. E. Scuseria, M. A. Robb, J. R. Cheeseman, G. Scalmani, V. Barone, B. Mennucci, G. A. Petersson, H. Nakatsuji, M. Caricato, X. Li, H. P. Hratchian, A. F. Izmaylov, J. Bloino, G. Zheng, J. L. Sonnenberg, M. Hada, M. Ehara, K. Toyota, R. Fukuda, J. Hasegawa, M. Ishida, T. Nakajima, Y. Honda, O. Kitao, H. Nakai, T. Vreven, J. A. Montgomery, Jr., J. E. Peralta, F. Ogliaro, M. Bearpark, J. J. Heyd, E. Brothers, K. N. Kudin, V. N. Staroverov, R. Kobayashi, J. Normand, K. Raghavachari, A. Rendell, J. C. Burant, S. S. Iyengar, J. Tomasi, M. Cossi, N. Rega, J. M. Millam, M. Klene, J. E. Knox, J. B. Cross, V. Bakken, C. Adamo, J. Jaramillo, R. Gomperts, R. E. Stratmann, O. Yazyev, A. J. Austin, R. Cammi, C. Pomelli, J. W. Ochterski, R. L. Martin, K. Morokuma, V. G. Zakrzewski, G. A. Voth, P. Salvador, J. J. Dannenberg, S. Dapprich, A. D. Daniels, O. Farkas, J. B. Foresman, J. V. Ortiz, J. Cioslowski and D. J. Fox, *Gaussian 09*, Revision A.02. Gaussian, Inc., Wallingford CT, 2009.
- S9 E. B. Wilson, J. C. Decius, P. C. Cross, *Molecular Vibration*, McGraw-Hill: New York, 1955.

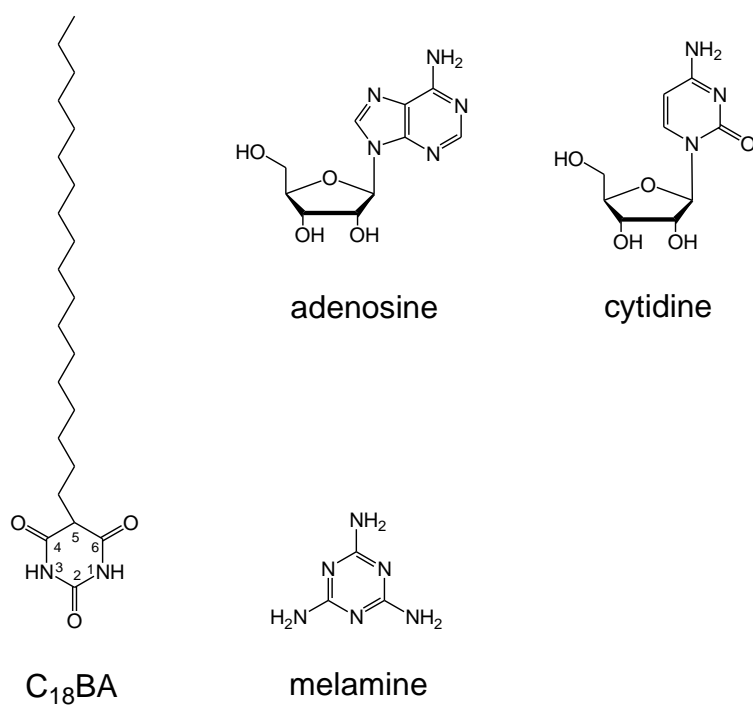


Fig. S1 Chemical structures of C₁₈BA amphiphile and related guest molecules.

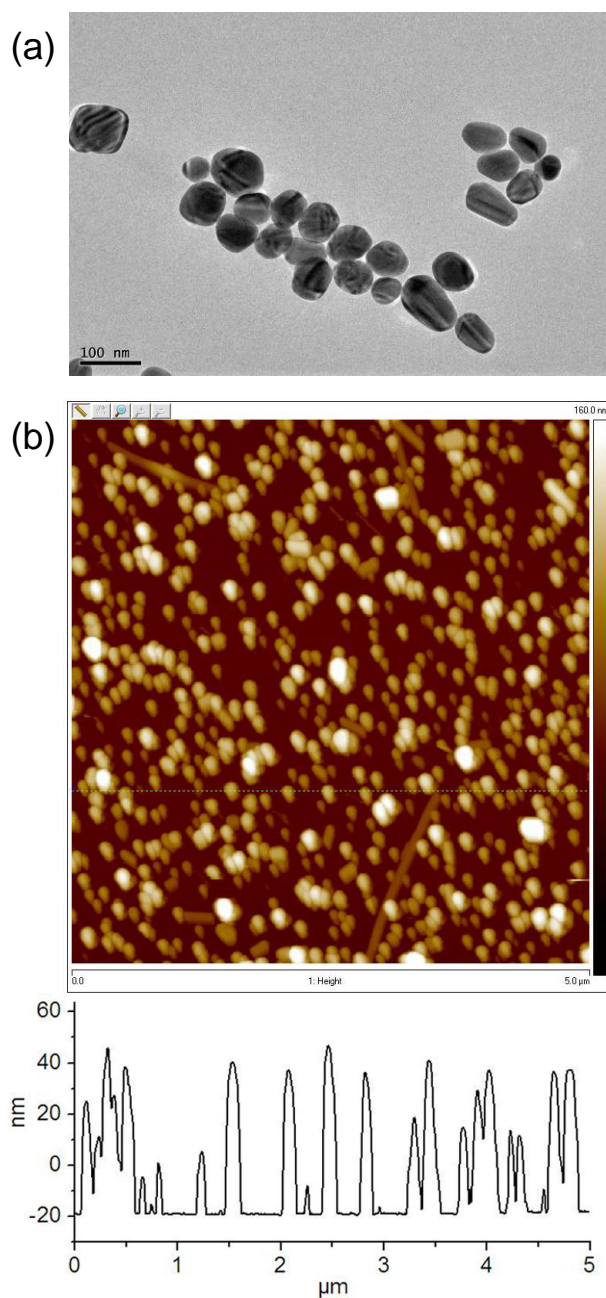


Fig. S2 (a) TEM image of AgNPs and (b) AFM image of AgNP-assembled silicon wafer pre-immobilized with APTMS. The flat silicon wafer with a relatively low roughness instead of glass plate was used for clear image.

The vertical dimensions of immobilized AgNPs on the silicon wafer were in the vicinity of 60 nm (b), which is consistent with the average diameters of as-synthesized AgNPs (a).

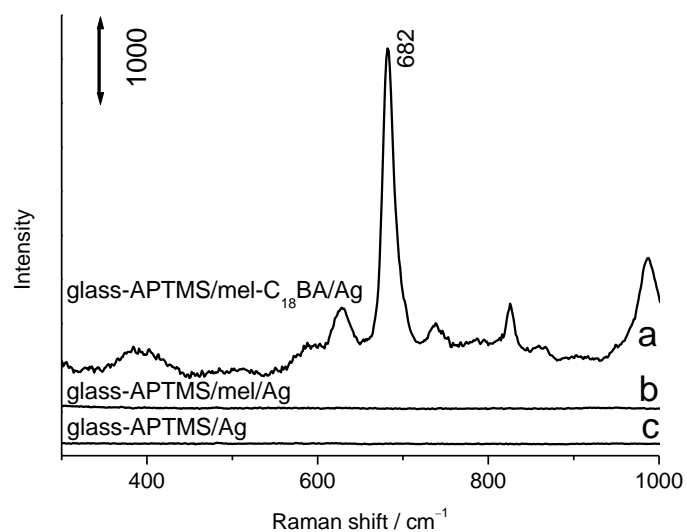


Fig. S3 SERS spectra of APTMS-modified smooth glass plates pulled from aqueous melamine subphase (1 mM) in the presence (a) and absence (b) of C₁₈BA LB monolayer followed by spreading AgNPs on the surface in comparison with (c) an APTMS-modified smooth glass plate after silver staining.

Melamine could not be adsorbed with the amino-functionalized glass plates. The detected SERS signals of melamine were owing to the molecular recognition with the C₁₈BA monolayer.

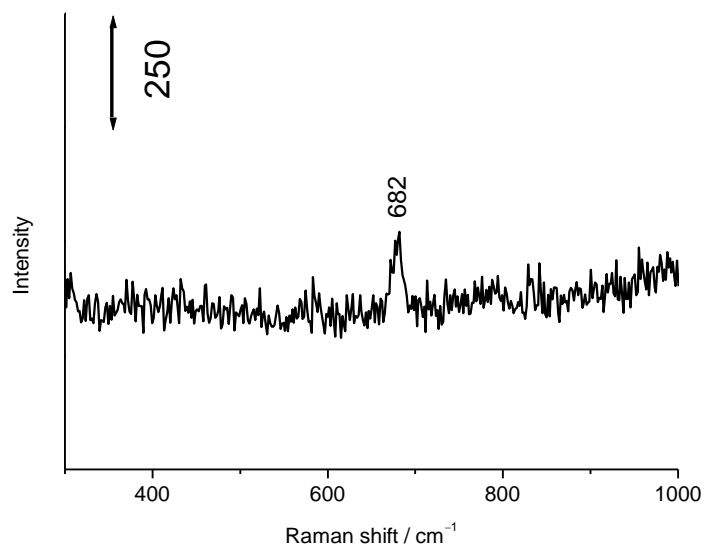


Fig. S4 Normal Raman spectrum of aqueous melamine solution.

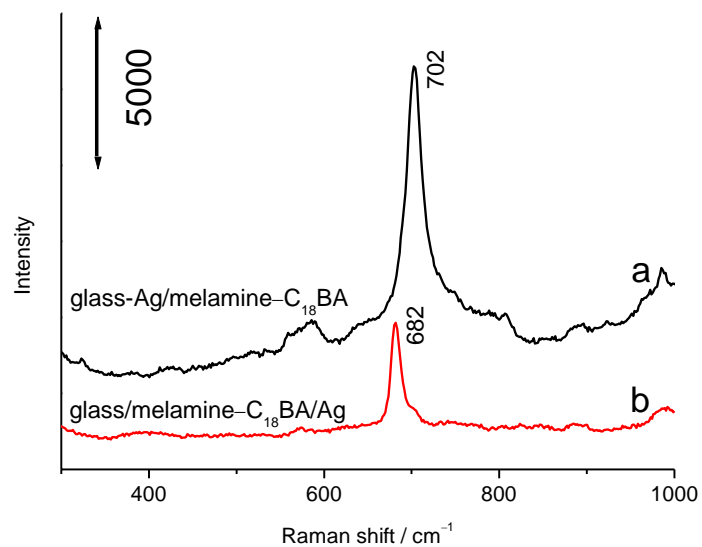


Fig. S5 Comparison of SERS spectra of C₁₈BA monolayers on aqueous melamine subphase (1 mM) transferred onto AgNP-assembled substrate (a) and smooth glass slide followed by spreading AgNPs on the surfaces of alkyl chains (b).

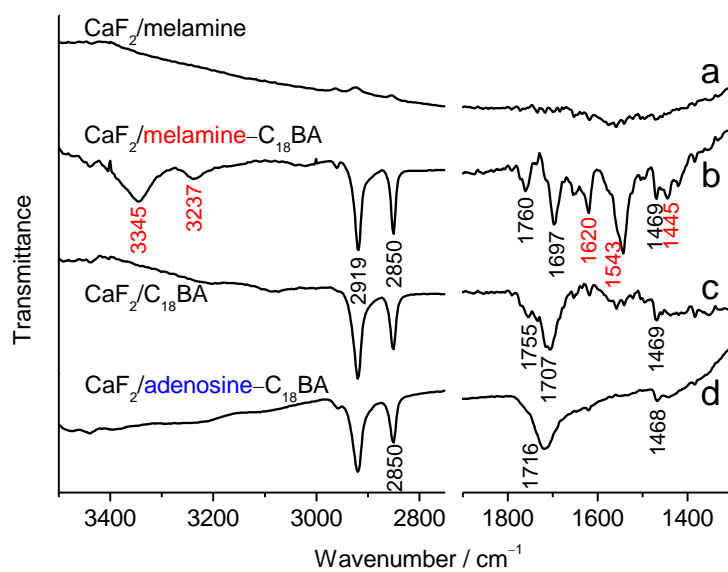


Fig. S6 FTIR spectra of CaF₂ substrates transferred from (a) aqueous melamine solution (1 mM) without C₁₈BA monolayer, (b) C₁₈BA monolayer on aqueous melamine subphase (1 mM), (c) C₁₈BA monolayer on pure water, and (d) C₁₈BA monolayer on aqueous adenosine subphase (1 mM). The peaks indicated in red were relevant to melamine.

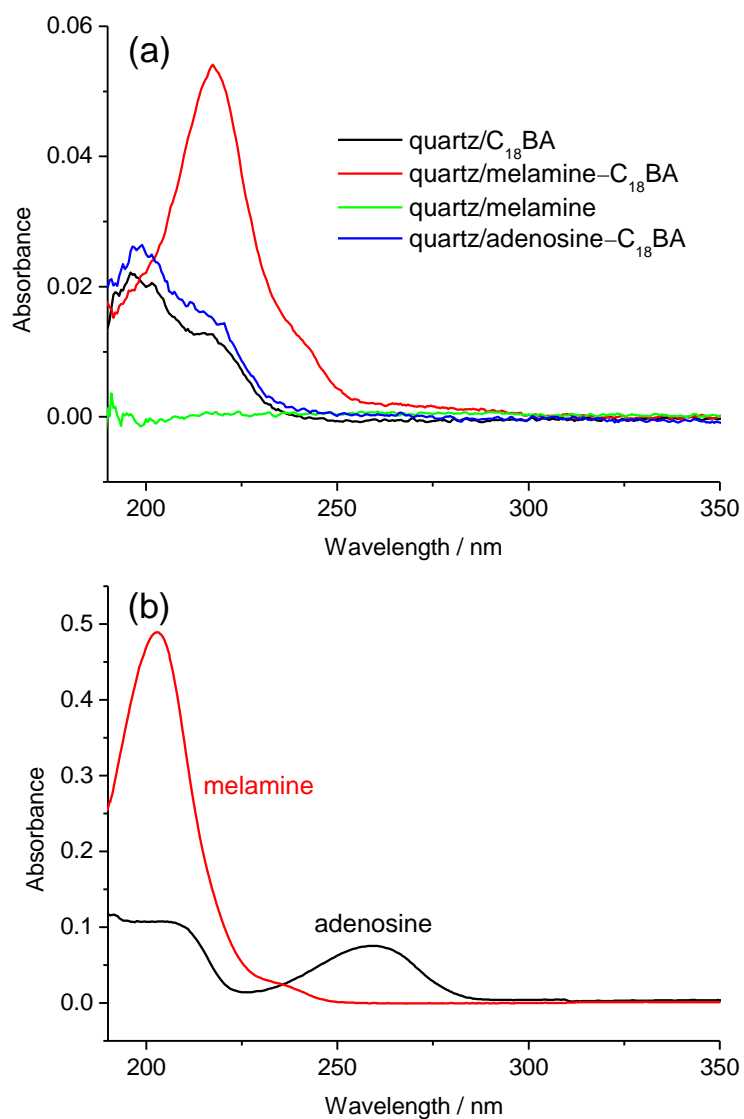


Fig. S7 UV-vis spectra of (a) quartz substrates transferred from C₁₈BA monolayer on pure water, aqueous melamine subphase solution (1 mM), aqueous adenosine subphase (1 mM), and aqueous melamine solution (1 mM) without C₁₈BA monolayer and (b) UV-vis spectra of aqueous melamine and adenosine solutions (1 mM).

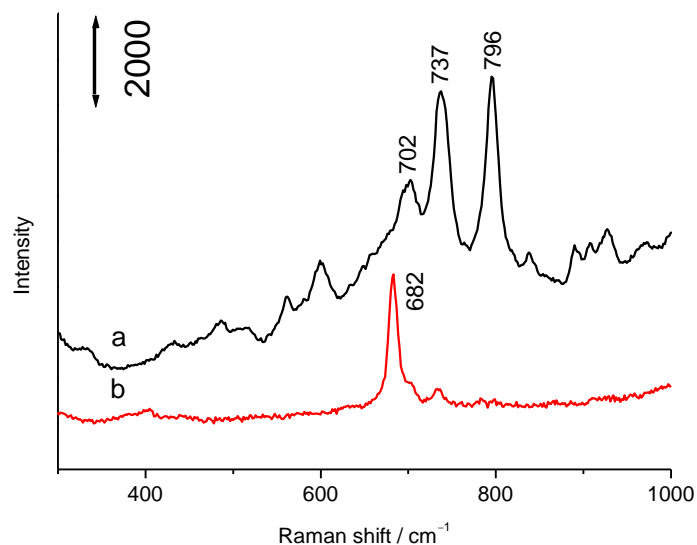


Fig. S8 SERS spectra of (a) an AgNP-assembled substrate dipped from aqueous subphase containing melamine, adenosine, and cytidine (1 mM for each guest) and (b) a C₁₈BA LB monolayer transferred from the mixed aqueous subphase onto a smooth glass slide followed by silver staining.

Recognition selectivity of the C₁₈BA monolayers was investigated with the ALINERS approach (Fig. S8). The AgNP-assembled substrate was pulled from mixed aqueous solution containing melamine, adenosine, and cytidine in the absence of C₁₈BA monolayer, and three SERS peaks at 702, 737, and 796 cm⁻¹ appeared due to the ring breathing modes of melamine, adenine, and cytosine, which indicates that the three kinds of nitrogen-containing heterocycles were readily adsorbed onto the AgNP-assembled substrate. A smooth glass plate was used to transfer the C₁₈BA monolayer from the mixed aqueous solution followed by silver staining, the SERS peak at 682 cm⁻¹ relevant to melamine was clearly observed, which indicates that the C₁₈BA monolayer had recognition selectivity of melamine over adenosine and cytidine. The commonly used SERS-active substrates for transfer of LB monolayers cannot yield reliable SERS signals of molecular recognition because of serious interference of adsorbed analytes.

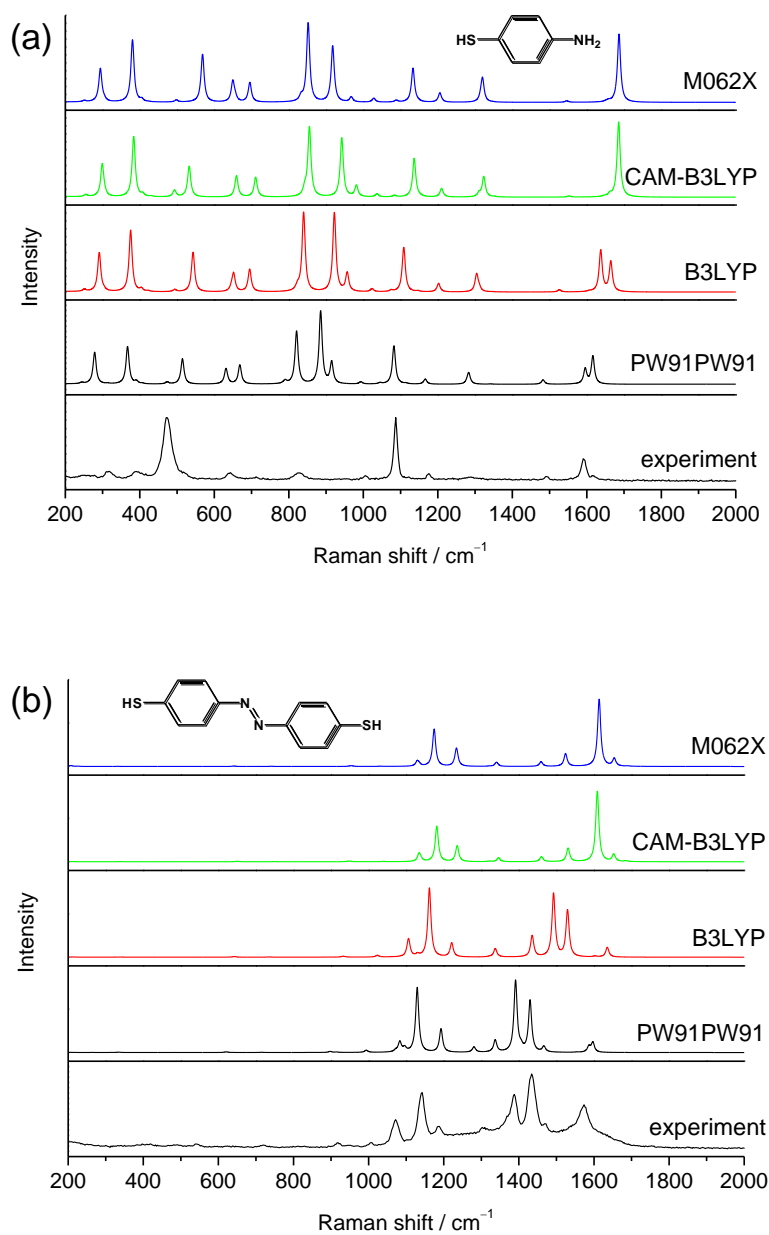


Fig. S1 Comparison of calculated normal Raman spectra using various methods of (a) *p*-aminothiophenol (PATP) and (b) 4,4'-dimercaptoazobenzene (DMAB) with experimental Raman spectra: (a) Raman spectrum of PATP powders; (b) SERS spectrum of PATP on AgNP-assembled glass substrate. The laser wavelength in the experiment was 532 nm.

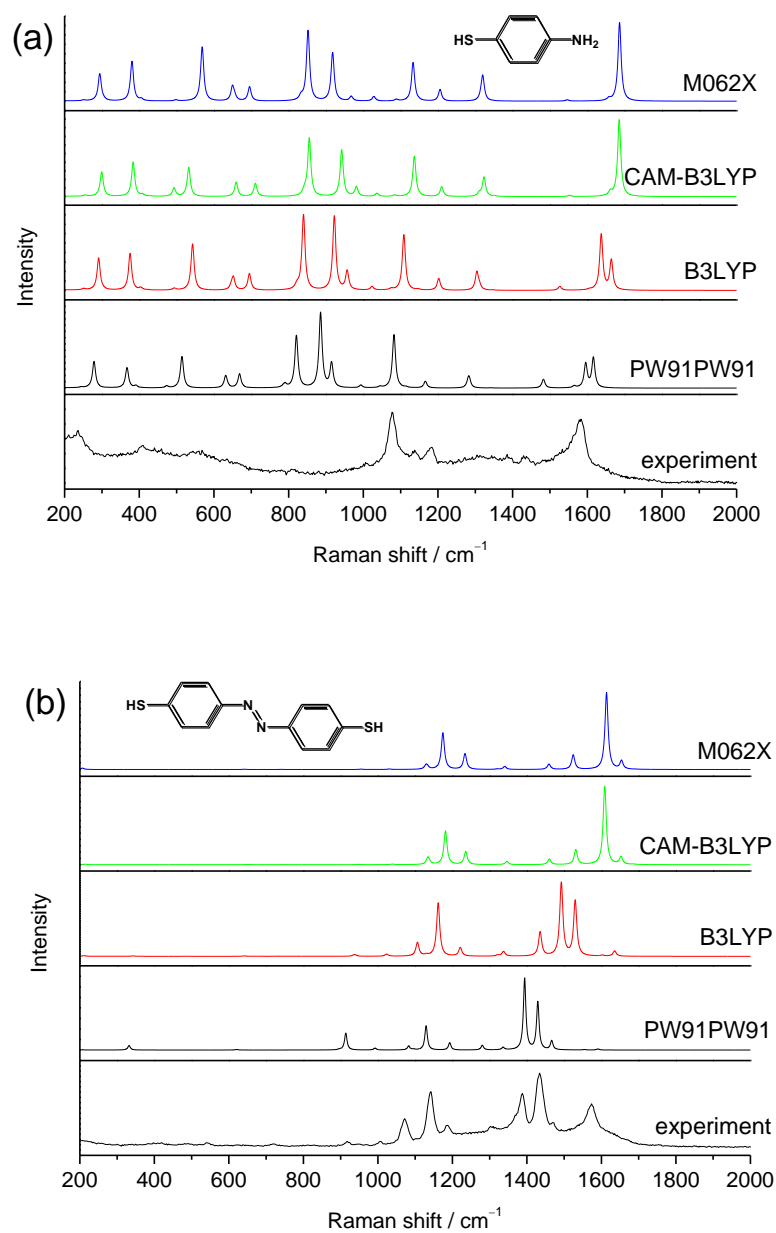


Fig. S2 Comparison of calculated pre-resonance Raman spectra at the excitation wavelength of 532 nm using various methods of (a) PATP and (b) DMAB with experimental Raman spectra: (a) SERS spectrum of PATP with stearic acid monolayer as a space layer; (b) SERS spectrum of PATP on AgNP-assembled glass substrate. The laser wavelength in the experiment was 532 nm.

Table S1 Calculation results of main Raman active modes of PATP by PW91PW91.

| normal Raman shift (cm^{-1}) | Raman scattering activity ($\text{\AA}^4/\text{amu}$) | pre-resonance Raman shift (cm^{-1}) | Raman scattering activity ($\text{\AA}^4/\text{amu}$) |
|--|--|---|--|
| 278.862 | 4.508 | 278.840 | 6.292 |
| 367.177 | 8.038 | 367.182 | 7.250 |
| 514.536 | 8.658 | 514.309 | 18.029 |
| 631.054 | 5.323 | 631.056 | 6.282 |
| 668.564 | 9.187 | 668.554 | 11.318 |
| 820.850 | 32.992 | 820.850 | 54.636 |
| 885.497 | 50.027 | 885.565 | 86.375 |
| 915.043 | 15.388 | 915.045 | 29.351 |
| 1082.204 | 33.967 | 1082.232 | 79.320 |
| 1166.255 | 4.882 | 1166.290 | 10.904 |
| 1280.142 | 2.419 | 1280.168 | 5.071 |
| 1283.194 | 11.185 | 1283.202 | 19.010 |
| 1482.495 | 5.7181 | 1482.509 | 19.6796 |
| 1595.694 | 22.3318 | 1595.71 | 59.5797 |
| 1616.287 | 41.9208 | 1616.29 | 75.6901 |

Table 2 Calculation results of main Raman active modes of DMAB by PW91PW91.

| normal Raman shift (cm^{-1}) | Raman scattering activity ($\text{\AA}^4/\text{amu}$) | pre-resonance Raman shift (cm^{-1}) | Raman scattering activity ($\text{\AA}^4/\text{amu}$) |
|--|--|---|--|
| 993.714 | 206.675 | 992.394 | 22599.383 |
| 1083.024 | 1094.317 | 1082.710 | 53906.205 |
| 1096.074 | 452.094 | 1096.070 | 8508.727 |
| 1129.373 | 7377.676 | 1129.411 | 349122.588 |
| 1192.753 | 2868.411 | 1192.829 | 114378.130 |
| 1280.507 | 703.088 | 1280.412 | 81330.533 |
| 1337.042 | 1708.426 | 1336.188 | 47599.545 |
| 1391.220 | 10643.010 | 1393.930 | *1434134.642 |
| 1406.023 | 576.883 | 1410.349 | 3.264 |
| 1429.898 | 7981.230 | 1429.237 | *1000000.237 |
| 1466.659 | 892.560 | 1466.536 | 197866.017 |
| 1586.411 | 1019.894 | 1554.588 | 9551.664 |
| 1597.024 | 1769.343 | 1590.773 | 26823.785 |

* The RSA in pre-resonance Raman spectra of the modes at 1391 and 1429 cm^{-1} were larger than the maximum limit that Gaussian output files could display. That means that their RSA values were larger than 999999. Therefore, we used 1000000 to represent the RSA value of the mode at 1429 cm^{-1} , which was the minimum value that could not display. The RSA ratio of the modes at 1429 to 1391 cm^{-1} was equal to the RSA ratio in normal Raman spectra.

By comparing the calculation results, we could conclude that the PW91PW91 density was more accurate in calculating Raman spectra of PATP and DMAB than other three methods. The B3LYP method provided right profiles of the Raman spectra, but the vibrational wavenumbers were always larger than the experimental results due to the inharmonic effects. Therefore, a factor of approximate 0.98 was needed for the wavenumbers of the Raman spectra obtained by the B3LYP method to scale down. Both CAM-B3LYP and M062X methods gave similar results, but none of them was consistent with the experimental results.

The calculated Raman spectrum of DMAB by PW91PW91 was very close to the experimental one, but the calculated Raman spectrum of PATP by the same method was not completely consistent with the experimental one. The most obvious difference was that two major intense Raman shifts at 820 and 885 cm^{-1} in the calculated spectra were difficult to match with the experimental spectra. Based on our calculations, the reason that there were only two intense vibrational modes in the experiment spectra was due to the pre-resonance effect triggered by the laser excitation. We compare the calculation results of normal Raman spectra and pre-resonance Raman spectra and find that the Raman scattering activities (RSA) of the two vibrational modes at 1082 and 1595 cm^{-1} increased by 2.33 and 2.67 times, respectively. The increased factors for the two modes were bigger than those for other vibrational modes including the shifts at 820 and 885 cm^{-1} . The two vibrational modes were coincident with the two intense peaks in the experimental spectra.